

ISSN 1678-3921

Journal homepage: www.embrapa.br/pab

For manuscript submission and journal contents,
access: www.scielo.br/pab

Silicon in cacao plants exposed to UV-B radiation





Abstract – The objective of this work was to evaluate silicon capacity to mitigate the damaging effects of UV-B radiation on cacao (*Theobroma cacao*) plants. For the experiment, homogeneous cacao plants produced from seeds collected from a clonal population were subjected to the following treatments: UVB- Si-, no UV-B exposure and no addition of Si (control); UV-B+ Si-, UV-B exposure of 3.0 kJ m⁻² per day and no addition of Si; and UV-B+ Si+, UV-B exposure of 3.0 kJ m⁻² per day and addition of 2.0 mmol L⁻¹ Si. The molybdenum blue technique was used to determine Si concentrations. For each selected plant, the following were determined: number of leaves; leaf area; root, stem, and leaf dry mass; anatomy of fully expanded leaves; gas exchange; chlorophyll *a* fluorescence; total soluble sugar concentrations using ethanol extract; and antioxidant enzyme activity. The plants showed a higher leaf and total biomass when treated with Si, as well as lower concentrations of chlorophyll, carotenoids, anthocyanins, flavonoids, and polyphenols under UV-B radiation. Si inhibits the net CO₂ assimilation rate and the dark mitochondrial respiration rate. Therefore, Si application on cacao plants mitigates the damaging effects of UV-B, reduces carbon consumption through cellular respiration, and decreases the production of UV-B-absorbing compounds.

Index terms: oxidative stress, photosynthesis, plant anatomy, plant growth, ultraviolet radiation.

Silício em plantas de cacau expostas à radiação UV-B


Resumo – O objetivo deste trabalho foi avaliar a capacidade do silício em mitigar os efeitos nocivos da radiação UV-B em plantas de cacau (*Theobroma cacao*). Para o experimento, plantas homogêneas de cacau produzidas de sementes coletadas de uma população clonal foram submetidas aos seguintes tratamentos: UV-B- Si-, sem exposição à UV-B e sem adição de Si (controle); UV-B+ Si-, exposição à UV-B a 3,0 kJ m⁻² por dia e sem adição de Si; e UV-B+ Si+, exposição à UV-B a 3,0 kJ m⁻² por dia e adição de 2.0 mmol L⁻¹ de Si. Utilizou-se a técnica azul de molibdênio para determinar as concentrações de Si. Para cada planta selecionada, foram determinados: número de folhas; área foliar; massa seca de raízes, caules e folhas; anatomia das folhas totalmente expandidas; trocas gasosas; fluorescência da clorofila *a*; concentrações de açúcares solúveis totais com uso de extrato etanólico; e atividade das enzimas antioxidantes. As plantas apresentaram maior biomassa foliar e total quando tratadas com Si, bem como menores concentrações de clorofila, carotenoides, antocianinas, flavonoides e polifenóis sob radiação UV-B. O Si inibe a taxa de assimilação líquida de CO₂ e a taxa de respiração mitocondrial no escuro. Portanto, a aplicação de Si em cacauzeiros atenua os efeitos nocivos da UV-B, reduz o consumo de carbono pela respiração celular e diminui a produção de compostos absorvedores de UV-B.

Termos para indexação: estresse oxidativo, fotossíntese, anatomia vegetal, crescimento vegetal, radiação ultravioleta.

Leonardo Valandro Zanetti⁽¹⁾ ,
Elias Terra Werner⁽²⁾ ,
Geraldo Rogério Faustini Cuzzuol⁽¹⁾  and
Camilla Rozindo Dias Milanez⁽¹⁾ 

⁽¹⁾ Universidade Federal do Espírito Santo,
Centro de Ciências Humanas e Naturais,
Departamento de Ciências Biológicas, CEP
29075-910 Vitória, ES, Brazil.
E-mail: valandroleo@gmail.com,
gcuzzuol@gmail.com,
camilla.milanez@gmail.com

⁽²⁾ Universidade Federal do Espírito Santo,
Centro de Ciências Exatas, Naturais e da
Saúde, Departamento de Biologia, CEP
29500-000 Alegre, ES, Brazil.
E-mail: elias.werner@ufes.br

 Corresponding author

Received

August 09, 2022

Accepted

February 06, 2023

How to cite

ZANETTI, L.V.; WERNER, E.T.; CUZZUOL, G.R.F.; MILANEZ, C.R.D. Silicon in cacao plants exposed to UV-B radiation. **Pesquisa Agropecuária Brasileira**, v.58, e03083, 2023. DOI: <https://doi.org/10.1590/S1678-3921.pab2023.v58.03083>.

Introduction

The Catongo cacao (*Theobroma cacao* L.) genotype is well-known for the good quality of its seeds, which provide the raw material necessary to obtain low-acidity fine chocolates with a high-quality flavor (Bonino, 2013).

Although cacao is usually grown under temporary or permanent shading, the cultivation of the crop under full sunlight conditions has been expanding (Lennon et al., 2021). However, a high exposure to ultraviolet-B (UV-B) radiation should be carefully evaluated since, depending on its levels, the effects on plant growth can be negative (Kakani et al., 2003b; Yao & Liu, 2006) or even positive (Cuzzuol et al., 2020). Yao & Liu (2006) and Cuzzuol et al. (2020), for example, found that, at 14.33 and 4.2 kJ m⁻² per day, respectively, UV-B radiation inhibited and promoted plant development.

At the anatomical level, the negative effects of UV-B include the thickening of the adaxial epidermis, palisade parenchyma, and spongy parenchyma, culminating in limb thickness (Verdaguer et al., 2012). In addition, UV-B reduces stomatal density in sensitive species (Kakani et al., 2003a) and can affect net CO₂ assimilation rate, stomatal conductance, transpiration, water-use efficiency (net CO₂ assimilation rate/transpiration), CO₂ concentration in intercellular air spaces, and the efficiency in trapping excitation energy (F_v'/F_m') of photosystem II (PSII) open reaction centers (Yao & Liu, 2006; Cuzzuol et al., 2020).

A few studies have also shown that UV-B affects plant cell walls, which represent the largest reservoir of carbon in plants and in the biosphere, playing a key role in carbon cycling (Schädel et al., 2010). In herbaceous species of the Arctic region, Ruhland et al. (2005) found that UV-B increased the content of phenolic compounds in the cell wall structure of leaf tissues, whereas, in the tropical species *Paubrasilia echinata* (Lam.) Gagnon, H.C.Lima & G.P.Lewis, Cuzzuol et al. (2020) concluded that UV-B stimulated lignification in the leaves. In another study, Messenger et al. (2009) highlighted that UV-B drove the aerobic production of methane and pectin in plant tissues, resulting in cell wall loosening. However, other possible effects of UV on lignin and mucilage content are still unknown, showing the need for further research on cellular tissues.

Plant sensitivity to UV-B has been associated with the balance between oxidant activity and antioxidant

potential (Kataria et al., 2014). Under a long period of UV-B exposure, plants produce more reactive oxygen species (ROS) such as hydrogen peroxide (H₂O₂) (Kataria et al., 2014), a potent agent of lipid peroxidation detected through an increased malondialdehyde (MDA) concentration (Asada, 1999). ROS can be presented as superoxide radicals (O₂⁻), hydroxyl radicals (·OH), and singlet oxygen (¹O₂), oxidizing not only lipids, but also proteins and nucleic acids (Hideg et al., 2013). In this scenario, antioxidant components have been evaluated as to plant protection against UV-B oxidant effects through non-enzymatic and enzymatic mechanisms (Martínez-Lüscher et al., 2015).

Non-enzymatic mechanisms consist of substances accumulated on the upper surface of the leaf epidermis, acting as UV absorbers and preventing the formation of ROS (Hideg et al., 2013), among which flavonoids (Ruuholta et al., 2018), anthocyanins, and carotenoids stand out (Sankari et al., 2017). Another form of non-enzymatic defense consists in plants accumulating sugars that function as ROS scavengers (Mengarda et al., 2012).

Enzymatic antioxidant mechanisms involve the activity of superoxide dismutase (SOD, EC 1.15.1.1), ascorbate peroxidase (APX, EC 1.11.1.11), catalase (CAT, EC 1.11.1.6), and other enzymes (Asada, 1999). According to Martínez et al. (2001), SOD is the first line of defense against radicals, eliminating O₂⁻. The authors added that this enzymatic activity converts hydrogen peroxide into H₂O and O₂ in the peroxisomes through CAT or in the chloroplasts through APX, showing how the antioxidant systems play an important role in protecting plants against the negative effects of oxidative stress.

In a pioneering study with cacao, Zanetti et al. (2016) observed that the foliar application of Si mitigated UV-B oxidative damages. The mechanism behind this mitigation was related to net CO₂ assimilation rate, water use efficiency, and CO₂ concentration in the intercellular air spaces. Yaghubi et al. (2016), Zanetti et al. (2016), and Feng et al. (2010) concluded that Si application also protects plants against different types of stresses, such as salinity in strawberry (*Fragaria × ananassa* Duch.), water deficit in cacao, and heavy metal contamination in cucumber (*Cucumis sativus* L.), respectively. However, although abundantly present in the soil, Si concentration differs among soil types and

plant species, occurring mainly in the form of silicates (Epstein & Bloom, 2006).

The objective of this work was to evaluate silicon capacity to mitigate the damaging effects of UV-B radiation on cacao plants.

Materials and Methods

Seminal cacao plants of the Catongo genotype were produced using seeds from the same fruit of a clonal population, belonging to Comissão Executiva do Plano da Lavoura Cacaueira, located in the municipality of Linhares, in the state of Espírito Santo, Brazil (19°23'48"S, 40°03'42"W). The seeds were germinated in plastic trays containing filter paper and water, which were kept in a greenhouse under natural temperature, humidity, and photoperiod. A 50% black net was used to provide shade. The seeds with a visible root protrusion on the third day of germination were transferred to 290 mL polycarbonate tubes containing the Forth commercial substrate (Forth Jardim, Cerquilha, SP, Brazil) and kept in the LI15 growth chamber (Sheldon Manufacturing Inc., Cornelius, Oregon, USA) set to a photoperiod of 12 hours, temperature of 27°C, and relative humidity of 60%. Four 32 W white lamps (F32T8/SP41/ECO, General Electric, Boston, MA, USA) provided 150 $\mu\text{mol m}^{-2} \text{s}^{-1}$ photosynthetic photon flux density (PPFD). Every 15 days, the seedlings received 50 mL of the nutrient solution, at pH 6.2, proposed by Hoagland & Arnon (1950).

After 55 days, homogeneous plants, with 12 ± 2 cm in length and 7 ± 2 leaves, were selected for analysis. The experimental design was completely randomized with five plants per treatment kept in the same growth chamber under the previously described setup. The plants were subjected to the following three treatments: UV-B- Si-, no UV-B exposure and no addition of Si (control); UV-B+ Si-, UV-B exposure of 3.0 kJ m^{-2} per day and no addition of Si; and UV-B+ Si+, UV-B exposure of 3.0 kJ m^{-2} per day and addition of 2.0 mmol L^{-1} Si. Every 15 days, 50 mL of plain nutrient solution with Na_2HPO_4 were added to UV-B- Si- and UV-B+ Si-, whereas 50 mL of plain nutrient solution with 2.0 mmol L^{-1} Si as Na_2SiO_3 and H_2PO_4 were added to UV-B+ Si+. The aim was to balance the additional Na and P among treatments due to the use of Na_2SiO_3 (Ming et al., 2012).

After 15 days of Si application, the plants in the growth chamber were put on two shelves according to the treatments they were subjected to. Those under UVB+ Si- and UVB+ Si+ were put on the upper shelf in order to be exposed to two G15T8E lamps with an emission range of 280–360 nm and peak at 306 nm (Sankyo Denki, Kanagawa, Japan), positioned 30 cm above the plants; monitoring was carried out weekly using the 3414F ultraviolet light meter (Spectrum Technologies, Inc., Aurora, Illinois, USA). The plants under UVB- Si- were put on the lower shelf, protected from UV-B using a foam board.

Over 42 days, the plants exposed to UV radiation received 15 min per day of 5.5 $\mu\text{mol m}^{-2} \text{s}^{-1}$ UV-B intensity, corresponding to 3.0 kJ m^{-2} per day. This level was based on that between 2.0 and 12 kJ m^{-2} per day registered during spring in different regions of Earth's surface (Forster et al., 2011); the lower range was adopted because cacao is widely cultivated under trees, where the exposure to UV-B is lower. Every day, water was supplied up to 80% of the field capacity of the substrate, based on its mass. This limit was used to prevent Si leaching.

At the end of the experiment, photosynthesis, Si concentration in the substrate and leaf, growth measurement, leaf anatomy, and biochemical traits were determined. Photosynthesis was measured on fully-expanded apical leaves of the second and third nodes. For this, the leaves were removed, frozen, lyophilized, and ground for the biochemical analysis of pigments, enzymes, and molecules of the primary and secondary metabolism. Other leaves were used for Si content determination and anatomical analysis.

The modified molybdenum blue technique was used to determine Si concentration in substrates and leaves (Korndörfer et al., 2004). In the case of substrates, the material was oven-dried, at 60°C, until reaching a constant mass. Samples of 10 g of dry substrate were then sifted through a 2.0 mm mesh and put in a 500 mL beaker, to which 100 mL of 0.5 mol L^{-1} acetic acid were added. The mixture was shaken at 50 rpm for 1 hour in the GT-201BD horizontal shaker (Global Trade Technology, Jaboticabal, São Paulo, Brazil) and left to rest for 12 hours, after which the suspension was filtered and left to rest for another 12 hours. Then, a sample of 10 mL was collected, to which 1.0 mL sulfomolybdic solution (75 g L^{-1}) was added. The obtained solution was homogenized manually, receiving 2.0 mL oxalic

acid (75 g L⁻¹) after 10 min and 10 mL ascorbic acid (3.0 g L⁻¹) after 5 min; after each addition, the solution was homogenized manually again. The mixture was left to rest for 1 hour and, afterwards, analyzed in the Genesys 10S UVvis spectrophotometer (Thermo Fisher Scientific, Waltham, MA, USA) with an optical density at 660 nm. All absorbance measurements were carried out using the same spectrophotometer.

To quantify Si content in the leaves, the material was washed in deionized water, oven dried at 60°C, and ground in the TE-350 ball mill (TECNAL, Piracicaba, SP, Brazil). For each treatment, five 25 mg samples of the ground material were put in 15 mL falcon tubes to be digested. The tubes, which received 500 µL H₂O₂ (30 volumes) and 750 µL NaOH (500 g L⁻¹), were immersed in a water bath, at 90°C, where they were shaken for 1 hour using the SL-153/30 magnetic shaker (Solab: Equipamentos para Laboratórios, Piracicaba, SP, Brazil), followed by autoclaving at 123°C, under 1.5 atm, for 1 hour in the CS-30 equipment (Primatec Equipamentos, Itu, SP, Brazil). A volume of 11.25 mL ultrapure water was added to the digested extract, and the mixture was left to rest for 12 hours. A 500 µL aliquot of the supernatant was mixed with 4.5 mL ultrapure water, 0.5 mL HCl (1:1), and 0.5 mL ammonium molybdate (100 g L⁻¹), to which 0.5 mL oxalic acid (75 g L⁻¹) and 2.5 mL of ascorbic acid (3.0 g L⁻¹) were added after 10 and 5 min, respectively. The mixture was left to rest for 1 hour and then subjected to an optical density reading at 660 nm using the spectrophotometer. The standards for the calibration curve (0 to 8.0 mg L⁻¹ Si) were prepared using a 1.0 g L⁻¹ Si solution (Merck & Co. Inc., Rahway, NJ, USA).

At the end of the experiment, leaf number, leaf area, and root, shoot, and leaf dry mass (RDM, SDM, and LDM, respectively) were determined. Leaf area was measured with the LI-3100 Area Meter imaging scanner (LI-COR Biosciences, Lincoln, Nebraska, USA). Dry mass was obtained using plant material oven-dried at 60°C until reaching a constant mass. Based on the results, specific leaf area (SLA = leaf area/LDM), unit leaf area (ULA = leaf area/leaf number), leaf area ratio (LAR = leaf area/total dry mass), and the root:shoot ratio (RDM/SDM) were calculated according to Lambers & Poorter (1992).

Anatomic analyses were performed under proper phytosanitary conditions using fully expanded leaves

of the second node from the apex of the orthotropic axis. Samples were fixed in formalin-acetic acid-alcohol as proposed by Johansen (1940), kept in this solution for 48 hours, stored in ethyl alcohol 70%, and then subjected to increasing concentrations of ethanol (70, 90, 95, and 100%) for dehydration. The obtained material was embedded in hydroxyethyl methacrylate (Leica, Wetzlar, Germany). The resin blocks were cross-sectioned at a thickness of 8.0 to 10 µm using a rotating microtome, starting at the median portion of the leaf blade. Adaxial epidermis, abaxial epidermis, palisade parenchyma, and spongy parenchyma were measured. Stomatal density (number of stomata per square millimeter) was calculated from abaxial leaf epidermal impressions prepared with the Super Bonder instant adhesive (Loctite, Henkel, Düsseldorf, Germany) on glass slides. The samples were photo-documented using the Nikon Eclipse 50i photomicroscope and the Nikon NIS-Elements imaging software (Nikon Tec Corporation, Tokyo, Japan). Quantitative analyzes were conducted with the ImageJ1 software (Schneider et al., 2012).

Using fully expanded leaves of the second and third apical node, gas exchange and chlorophyll *a* fluorescence were measured with the LI-6400XT infrared gas analyzer coupled with the LI-6400-02B LED red/blue light source and the LI-6400-40 fluorometer (LI-COR Biosciences, Lincoln, NE, USA). The system was maintained under a constant irradiance of 500 µmol m⁻² s⁻¹ and 400 µmol mol⁻¹ CO₂, at 27°C. Net CO₂ assimilation rate, stomatal conductance, CO₂ concentration in the intercellular air spaces, transpiration, and water-use efficiency (net CO₂ assimilation rate/transpiration) were measured from 08:00 to 10:00 am. Dark respiration was deducted from the photosynthetic curves of light response (net CO₂ assimilation rate/PPFD) in the photon range of 0 to 1,500 µmol m⁻² s⁻¹, at 27°C. Curves were normalized as proposed by Lobo et al. (2013). The model of the data was adjusted using a non-linear regression (minimum quadratic difference) solved in the Microsoft Excel Solver software (Microsoft Corporation, Redmond, WA, USA).

For chlorophyll *a* fluorescence determination, leaves were acclimatized in the dark for 30 min and then exposed to a faint red-distant pulse of light of 0.03 µmol m⁻² s⁻¹ in order to determine the initial fluorescence yield in dark-adapted samples (F₀). Then,

an 8,000 $\mu\text{mol m}^{-2} \text{s}^{-1}$ saturating light pulse was applied for 0.8 s to estimate maximal fluorescence yield (F_m), maximum fluorescence in light-adapted samples (F_m'), fluorescence yield at the stationary state (F_s), and minimum fluorescence in the dark with all reaction centers open (F_0'). The photochemical extinction coefficient was estimated according to DaMatta et al. (2002) and Lima et al. (2002), using their equations of photochemical [$\text{qP} = (F_m' - F_s) / (F_m' - F_0')$] and non-photochemical [$\text{NPQ} = (F_m - F_m') / (F_m - F_0')$] extinction. The capture efficiency of excitation energy of PSII open reaction centers was determined using the following equation of Logan et al. (2007): [$F_v' / F_m' = (F_m' - F_0') / F_m'$].

Single extracts of five plants per treatment were prepared in order to determine chlorophyll content and UVB-absorbing compounds. Each extract of 18 mg lyophilized leaf tissue was macerated and left in 95% ethanol for 24 hours, in the dark, at 8°C. After ethanol extraction, the mixture was centrifuged at $1,450 \times g$, at 4°C, for 20 min. The supernatant obtained after centrifugation was the extract analyzed at 470, 648, and 664 nm using the spectrophotometer. The results were subjected to the equation of Lichtenthaler & Buschmann (2001) in order to determine chlorophyll *a*, chlorophyll *b*, and carotenoid concentrations. A modified Folin-Ciocalteu reaction developed from the methodology of Singleton & Rossi (1965) was used to determine soluble phenolic compounds. The reaction consisted of a mixture of 200 μL ethanolic extract with 200 μL Folin-Ciocalteu reagent agitated for 4 min at 25°C. The mixture received 1.0 mL Na_2CO_3 (15%) and was left to rest for 2 hours. Then, absorbance was read at 760 nm. Polyphenol content was determined using a standard curve of gallic acid from 0 to 60 μg , and the results were expressed in milligrams of gallic acid equivalent per gram of dry mass. Flavonoid content was estimated by the aluminum chloride colorimetric method described by Park et al. (1998), which uses a reaction consisting of 500 μL ethanolic extract, 100 μL aluminum chloride (10%), 100 μL potassium acetate (1.0 mol L^{-1}), and 4.3 mL distilled water. After homogenization, the mixture was left to react for 30 min at 25°C. Then, absorbance was read at 428 nm in the spectrophotometer. A standard curve from 0 to 100 $\mu\text{g mL}^{-1}$ quercetin was used. Anthocyanin content was obtained with a modified method based on the methodology of Beggs & Wellmann (1994), in which

the used reaction consisted of 1.5 mL extract subjected to 15 μL HCl (1%) and kept in the dark, at 4°C, for 24 hours. Absorbance was read at 535 nm, and the results were expressed in A_{535} per gram of dry mass.

Total soluble sugar concentration was determined using the phenol-sulfuric acid method of Dubois et al. (1956), at 490 nm, in the spectrophotometer. The results were expressed in standard glucose curve from 0 to 40 $\mu\text{g mL}^{-1}$ (Merck & Co. Inc., Rahway, NJ, USA).

Lignin content was determined through the method of Santos et al. (2008) using 150 mg dry leaf of each plant per treatment. To the analyzed sample, 10 mL of 50 mmol L^{-1} potassium-sodium phosphate buffer, at pH 7, were added. The mixture was then centrifuged at $2,616 \times g$ for 10 min, and the supernatant was discarded. The obtained pellet was washed using a sequence of different solutions: three times with 50 mmol L^{-1} phosphate buffer, at pH 7; three times with Triton buffer, at pH 7 (Thermo Fisher Scientific, Waltham, MA, USA); twice with NaCl buffer, at pH 7; twice with deionized water; and twice with 100% acetone. After chemical washing, the pellet was oven dried, at 60°C, for 24 hours. The resulting material was divided into batches of 50 mg, each receiving 1.2 mL thioglycolic acid and 6.0 mL of 2.0 mol L^{-1} HCl. The batches were incubated in a water bath, at 95°C, for 4 hours, centrifuged and washed with deionized water, and, then, each one of them received 7.0 mL of 0.5 mol L^{-1} NaOH. The mixture was incubated, at 30°C, for 18 hours under constant shaking, after which it was centrifuged and the supernatant was reserved. The obtained pellet was washed using 3.0 mL of 0.5 mol L^{-1} NaOH and centrifuged, receiving the reserved supernatant. The material was acidified with 1.8 mL HCl and left at 4°C for 12 hours, without shaking, in order to precipitate, and, then, washed using deionized water and centrifuged. The supernatant was discarded, and the centrifuged material was oven-dried, at 60°C, for 24 hours. Afterwards, the dried material was resuspended using 15 mL of 0.5 mol L^{-1} NaOH. At the concentrations of 0, 10, 20, 30, 40, 50, 100, 200, 300, 400, and 500 $\mu\text{g mL}^{-1}$, a lignin solution (Merck & Co. Inc., Rahway, NJ, USA) was used to plot the standard curve. The final material was analyzed at 280 nm with the spectrophotometer.

Mucilage extraction was carried out using the methodology of Ghanem et al. (2010), with modifications. For each treatment, five fully-expanded

leaves of the second and third apical node were immersed in absolute ethyl alcohol until complete depigmentation. The discolored material was oven-dried at 50°C and ground in a ball mill. Then, 3.0 mL water were added to 100 mg of the ground material. The mixture was subjected to ultrasound, at 35°C, for 15 min and, then, kept under constant agitation for 2 hours, after which it was centrifuged at $1,400 \times g$ for 5 min. The mucilage-rich supernatant was collected and stored at 4°C. The precipitate was resubjected twice to the process of mucilage extraction. The collected supernatants were added to 27 mL 95% ethanol, left to rest for 24 hours at 4°C, centrifuged again at $1,400 \times g$ for 5 min, and then discarded. The mucilage-rich precipitate was washed three times using 95% ethanol, after which it was vacuum-dried and weighed. Mucilage content was calculated by subtracting the initial weight from the final weight of the sample.

The antioxidant enzymes were extracted by liquid nitrogen from a sample of 50 mg lyophilized leaf tissue, which was homogenized using 0.1 mmol L⁻¹ potassium phosphate buffer at pH 6.8, 0.1 mmol L⁻¹ ethylenediaminetetraacetic acid (EDTANa₂), 10 mmol L⁻¹ ascorbic acid, and polyvinylpyrrolidone 1% (w/v). The homogenate was centrifuged at $12,000 \times g$ for 15 min at 4°C. Enzyme activities were determined from the supernatant (enzyme extract), whereas SOD activity was assessed according to the method of Giannopolitis & Ries (1977), in which the used reaction consisted of 3.0 mL of 50 mmol L⁻¹ NaH₂PO₄ buffer at pH 7.5, 13 mmol L⁻¹ methionine, 2.0 μmol L⁻¹ riboflavin, 0.1 mmol L⁻¹ EDTANa₂, 75 μmol L⁻¹ nitro blue tetrazolium, and 50 μL supernatant. The reaction occurred in a dark room under a white fluorescent 25 W lamp, at 25°C, for 10 min. Enzyme activity was defined as the amount of enzyme needed to inhibit 50% nitro tetrazolium reduction rate at a wavelength of 560 nm in the spectrophotometer, and the result was expressed in SOD per gram of dry mass. CAT activity was determined in the reaction of 100 μL of the supernatant added to 2.9 mL of 50 mmol L⁻¹ NaH₂PO₄ buffer, at pH 7.0, and 10 mmol L⁻¹ H₂O₂ (Aebi, 1984). The activity of this enzyme was calculated using the molar extinction coefficient of 36 L mol⁻¹ cm⁻¹ and expressed in μmol of H₂O₂ per minute per gram of dry mass. Absorbance decay was evaluated at 240 nm during 3 min at 25°C. APX activity was determined according to the method of Nakano & Asada (1981)

using a 100 μL aliquot of the enzyme extract, to which 2.9 mL of 50 mmol L⁻¹ NaH₂PO₄ buffer at pH 7.0, 0.1 mmol L⁻¹ EDTA Na², and 0.5 mmol L⁻¹ ascorbic acid were added; the reaction started with the addition of 0.2 mmol L⁻¹ H₂O₂. The molar extinction coefficient of 2.8 mmol L⁻¹ cm⁻¹ was used, and the results were expressed in μmol ascorbate per minute per gram of dry mass. Absorbance decay was evaluated at the optical absorption of 290 nm for 3 min at 25°C.

H₂O₂ and MDA contents were obtained using samples consisting of 40 mg extracts of fresh lyophilized leaf tissue of each plant per treatment, ground in liquid nitrogen with 2% polyvinylpyrrolidone, homogenized in 5.0 mL of 0.1% trichloroacetic acid, and centrifuged at $10,000 \times g$, at 4°C, for 10 min. To determine H₂O₂ content, the method of Alexieva et al. (2001) was used, in which 0.4 mL of 100 mmol L⁻¹ KH₂PO₄ buffer, at pH 7.0, and 1.6 mL of 1.0 mol L⁻¹ KI were added to 0.4 mL of the extract supernatant. The reaction was performed in the dark for 1 hour. A standard curve of 0–250 μmol L⁻¹ H₂O₂ was used. Absorbance rate was read at 390 nm using the spectrophotometer. For MDA content determination, the method of Buege & Aust (1978) was used, in which a 0.5 mL aliquot of the extract supernatant was added to the reaction medium of 0.5% 2-thiobarbituric acid (w/v) and 10% trichloroacetic acid (w/v). The mixture was incubated, at 95°C, for 30 min, subjected to flash freeze using ice in order to stop the reaction, and centrifuged at $10,000 \times g$; absorbance was read at 535 nm (A535) and 600 nm (A600). MDA content was calculated using the following equation of Du & Bramlage (1992): $MDA = [(A535 - A600) / 1.56] \times 10^{-5}$ cm⁻¹. The extinction coefficient used was 155 mmol L⁻¹ cm⁻¹, and the results were expressed in nmol per gram of dry mass.

The assumptions of independence of errors, normality of residuals, and homoscedasticity of variances of each variable were verified using the tests of Durbin-Watson, Shapiro-Wilk, and Bartlett, respectively. The assumptions for the one-way analysis of variance were met. The F-test, at 5% probability, was used. The means of the variables were compared by Tukey's test, also at 5% probability. The R, version 4.1.1, software (R Core Team, 2021) was used in the statistical analyzes, and the package ExpDes.pt, version 1.2.2, was installed.

Results and Discussion

Regarding Si concentration in the leaves and substrate, plants subjected to UV-B+ Si+ showed the highest values compared with all other treatments (Figure 1 A and B), whereas those under UV-B+ Si- showed the same Si concentration in the substrate (Figure 1 A) as those subjected to UV-B- Si-, but a significantly higher Si concentration in the leaves (Figure 1 B). The Si concentration in UV-B+ Si+ was equivalent to 1.21% (w/w) of the Si added in the substrate, indicating that cacao plants responded to the application of this element. According to Zanetti et al. (2016), concentrations above 1% indicate that plant roots are capable of capturing Si. In the present study, the results of Si concentration in the substrate and the leaves were not related to Si depletion in the substrate or to the increase of this element in the leaves of plants exposed to UV-B.

As to growth, UV-B reduced number of leaves, leaf area, ULA, LDM, LAR, and SLA, with leaf area being the most affected, inducing leaf changes such as necrosis, distortion, tanning, and abscission of newly emerged leaves (Figure 2). However, UV-B and Si did not affect RDM, SDM, TDM, and the root:shoot ratio (Table 1). Kataria & Guruprasad (2014) also reported reductions in leaf area and biomass due to UV-B effects in different varieties of *Amaranthus tricolor* L. In the present study, biomass losses decreased with the increase in LDM caused by Si application, which maintained TDM close to that of that plants that were not exposed to UV-B. This was also observed for wheat (*Triticum aestivum* L.) plants under UV-B exposure (Yao et al., 2011).

UV-B and Si did not influence leaf anatomy variables (Table 2). Although thickening seems to be a mechanism of protection of photosynthetic tissues (Verdaguer et al., 2012), under UV-B, only the palisade parenchyma and abaxial epidermis showed an increased thickness. This is an indicative that cacao may have other intrinsic protection mechanisms against radiation such as the presence of trichomes and mucilage (Nakayama et al., 1996). Contrastingly, for white clover (*Trifolium repens* L.), Hofmann & Campbell (2012) did not observe changes in leaf thickness under long periods of UV-B exposure.

The concentrations of chlorophyll *a*, chlorophyll *b*, carotenoids, anthocyanins, flavonoids, and polyphenols were lower in plants subjected to treatments UV-B+ Si+

and UV-B- Si- (Table 3). Although UV-B has degrading effects on chloroplast pigments (Kakani et al., 2003b), the higher concentrations found in UV-B+ Si- plants can be interpreted as an acclimation response to this radiation, as observed in *Arabidopsis thaliana* Schur (Biswas & Jansen, 2012). When compared with plants solely exposed to radiation (UVB+ Si-), cacao plants subjected to UV-B+ Si+ had lower concentrations of chlorophyll *a*, chlorophyll *b*, and carotenoids. This finding suggests that Si application increases plant

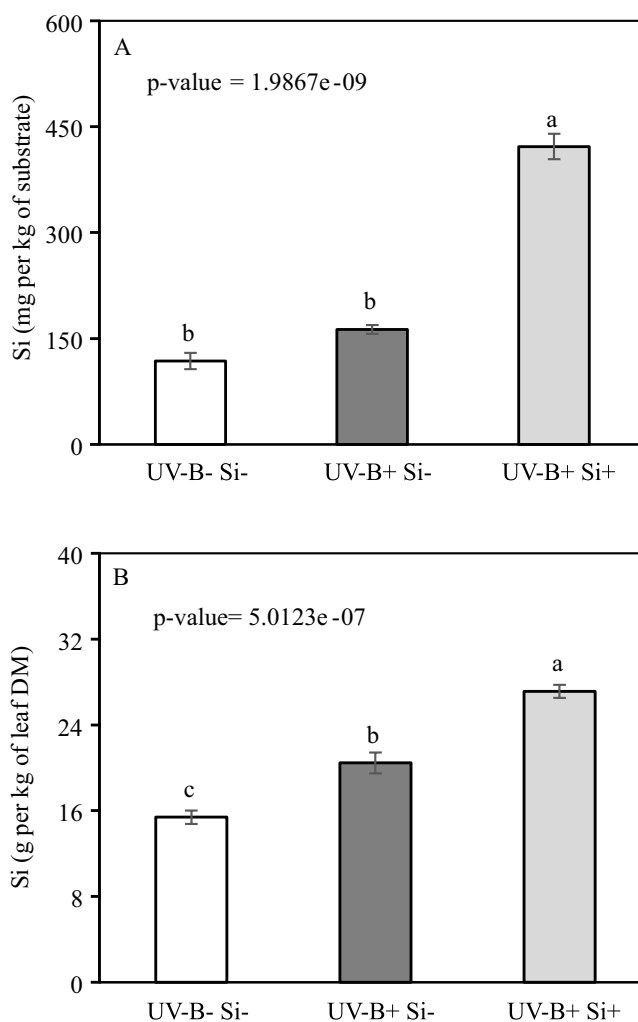


Figure 1. Effect of ultraviolet-B (UV-B) radiation and silicon on Si concentration in the substrate (A) and leaves (B) of plants of the Catongo cacao (*Theobroma cacao*) genotype. Equal letters do not differ by Tukey's test, at 5% probability. Bars represent the standard error of the mean (n = 5). UV-B-, 0.0 kJ m⁻² per day; UV-B+, 3.0 kJ m⁻² per day; Si-, 0.0 mmolL⁻¹; Si+, 2.0 mmolL⁻¹; and DM, dry matter.

tolerance to UV-B, allowing of the maintenance of chlorophyll and carotenoid concentrations at levels found in non-exposed plants, reflecting in the conservation of photosystems and photosynthesis rates.

Under UV-B+ Si-, cacao leaves showed high concentrations of UV-B-absorbing compounds, such as polyphenols, flavonoids, and anthocyanins, as also reported by Kakani et al. (2003b). These substances are considered the first barrier to UV-B penetration, functioning as protective screens and preventing damage to chloroplasts and other UV-B sensitive organelles (Yao et al., 2011). Studies investigating the behavior of soybean [*Glycine max* (L.) Merr.] and wheat exposed to UV-B verified that Si reduced the

concentration of UVB-absorbing compounds, which could indicate that the plant is under less stress and, therefore, saving energy (Yao et al., 2011).

Net CO₂ assimilation rate, stomatal conductance, and transpiration increased in the UV-B+ Si-treatment, explaining the lower water-use efficiency in plants under UV-B- Si-, which also presented a higher CO₂ concentration in intercellular air spaces and dark mitochondrial respiration rate (Figure 3). However, in the literature, few UV-B effects are positive, such as the stimulation of net CO₂ assimilation rate, whereas most of them are harmful to photosystems, decreasing photosynthesis (Kataria & Guruprasad, 2014). Plants exposed to UV-B showed higher values of stomatal conductance, indicating that this variable is responsible

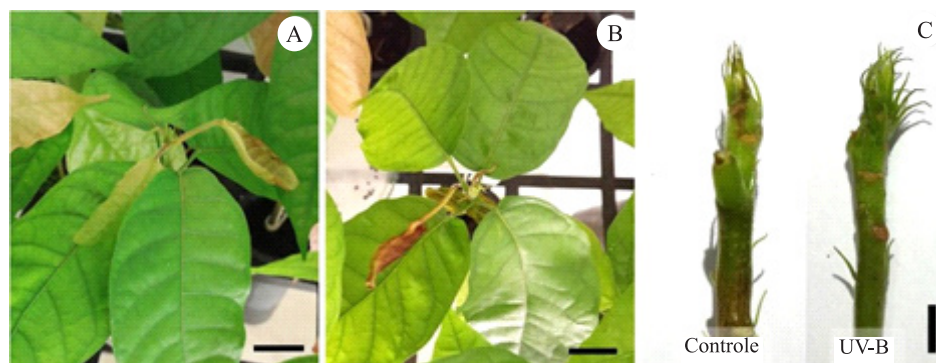


Figure 2. Effects of ultraviolet-B (UV-B) radiation on plants of the Catongo cacao (*Theobroma cacao*) genotype when not treated with silicon, showing: necrosis and leaf distortion (A), abscission of newly emerged leaves (B), and change in the number of stipules (C). UV-B-, 0.0 kJ m⁻² per day; and UV-B+, 3.0 kJ m⁻² per day. Bars measure 2.0 cm in A and B and 1.0 cm in C. Photos by Leonardo Valandro Zanetti.

Table 1. Effect of ultraviolet-B (UV-B) radiation and silicon on growth variables of plants of the Catongo cacao (*Theobroma cacao*) genotype⁽¹⁾.

Variable	UV-B- Si-	UV-B+ Si-	UV-B+ Si+	p-value
Leaf number (LN)	6.8a	5.4a	5.2a	0.040892
Leaf area (LA, cm ²)	297.46a	194.66b	196.66b	0.001199
Unit leaf area (ULA, cm ²)	44.13a	36.93b	35.90b	0.005369
Root dry mass (RDM, g)	0.608	0.640	0.655	0.66329
Shoot dry mass (SDM, g)	0.666	0.735	0.755	0.18736
Leaf dry mass (LDM, g)	0.695a	0.460b	0.503b	0.002531
Total dry mass (TDM, g)	1.969	1.835	1.913	0.37702
Root:shoot ratio (R:S, g g ⁻¹)	0.45334	0.53436	0.52108	0.1835
Leaf area ratio (LAR, cm ² g ⁻¹)	151.033a	106.1486b	102.8979b	0.0009155
Specific leaf area (SLA, cm ² g ⁻¹)	428.34a	421.66ab	391.17b	0.040753

⁽¹⁾Means (n = 5) followed by equal letters do not differ by Tukey's test, at 5% probability. ⁽²⁾UV-B-, 0.0 kJ m⁻² per day; UV-B+, 3.0 kJ m⁻² per day; Si-, 0.0 mmolL⁻¹; and Si+, 2.0 mmolL⁻¹.

for the greater absorption of CO₂. Contrastingly, plants not exposed to UV-B presented a reduced stomatal conductance, which, consequently, reduced net CO₂ assimilation rate and transpiration. However, these interactions between Si and UV-B on CO₂ assimilation were not observed for soybean and wheat plants (Yao et al., 2011). For grapevine (*Vitis vinifera* L.), Marínez-Lüscher et al. (2015) found a higher dark mitochondrial respiration rate under UV-B exposure, which is a common response of plants subjected to such growing conditions. An easier respiration of plants exposed to UV-B due to Si application implies a lower cost with photoassimilates, i.e., repairing damage to cellular components and UV-B defense substances.

Sucrose concentration did not differ due to different UV-B levels and Si addition. Plants subjected to UVB+ Si+ or UVB+ Si- showed the highest values of total sugar, reducing sugars, and lignin, whereas those under UV-B+ Si+ presented a discreet increase in these variables and the highest mucilage concentrations (Table 4). Therefore, cacao leaves exposed to UV-B and treated or not with Si showed significant high concentrations of total sugars and reducing sugars, agreeing with

the higher photosynthesis rates of the species. These concentrations also suggest cacao has a better osmotic adjustment (Kang et al., 2016), confirming the greater water-use efficiency observed in UVB+ Si+ when compared with the other treatments. Although there are no known reports in the literature on UV-B and Si increasing sugar content, Zhu et al. (2015) found that Si increased sucrose concentrations, suggesting gene expression and physiological adaptation.

Plants exposed to UV-B showed a higher lignin concentration, which acts as a barrier to radiation when accumulated in the leaf epidermis (Wong et al., 2022), indicating a defense response to this type of radiation. Regarding Si application, studies have shown that this element may be associated with a lignin-carbohydrate complex in epidermal cell walls of sorghum [*Sorghum bicolor* (L.) Moench] plants (Rivai et al., 2022). However, for cacao, Si had no influence on lignin deposition and on epidermis thickness. Under UV-B+ Si-, cacao leaves showed lower levels of mucilage, which protects the internal leaf structures against excessive radiation (Zanetti et al., 2016), indicating a loss of their initial defense. In this sense, Si combined

Table 2. Effects of ultraviolet-B (UV-B) radiation and silicon on leaf anatomy variables of plants of the Catongo cacao (*Theobroma cacao*) genotype⁽¹⁾.

Variable	UV-B- Si-	UV-B+ Si-	UV-B+ Si+	p-value
Adaxial epidermis thickness (µm)	19.71	19.97	19.45	0.83561
Abaxial epidermis thickness (µm)	12.81	12.50	13.08	0.46359
Palisade parenchyma thickness (µm)	25.54	28.68	28.09	0.13817
Spongy parenchyma thickness (µm)	21.99	21.04	18.94	0.21619
Blade thickness (µm)	80.06	82.20	79.25	0.58756
Stomatal density (n° per mm ²)	333.37	364.01	371.82	0.53327

⁽¹⁾Means (n = 5) followed by equal letters do not differ by Tukey's test, at 5% probability. UV-B-, 0.0 kJ m⁻² per day; UV-B+, 3.0 kJ m⁻² per day; Si-, 0.0 mmolL⁻¹; and Si+, 2.0 mmolL⁻¹.

Table 3. Effects of ultraviolet-B (UV-B) radiation and silicon on chlorophyll contents and UV-B-absorbent compounds (carotenoids, anthocyanins, flavonoids, and polyphenols) in leaves of plants of the Catongo cacao (*Theobroma cacao*) genotype⁽¹⁾.

Variable	UV-B- Si-	UV-B+ Si-	UV-B+ Si+	p-value
Chlorophyll a (mg g ⁻¹ DM)	2.95b	4.83a	3.66b	0.0016784
Chlorophyll b (mg g ⁻¹ DM)	0.91b	1.48a	1.01b	0.0016347
Carotenoids (mg g ⁻¹ DM)	0.77b	1.23a	0.87b	0.00089117
Anthocyanins (A _{535 nm} g ⁻¹ DM)	3.14b	5.27a	3.36b	0.00019462
Flavonoids (mg quercetin per gram of DM)	72.41b	113.70a	68.72b	2.3761e-05
Polyphenols (mg gallic acid per gram of DM)	30.67b	45.44a	27.58b	0.00033382

⁽¹⁾Means (n = 5) followed by equal letters do not differ by Tukey's test, at 5% probability. UV-B-, 0.0 kJ m⁻² per day; UV-B+, 3.0 kJ m⁻² per day; Si-, 0.0 mmolL⁻¹; Si+, 2.0 mmolL⁻¹; and DM, dry matter.

with UV-B was beneficial for cacao plants, increasing leaf mucilage concentration.

SOD and CAT activities were higher in plants subjected to UV-B+ Si+, but did not differ significantly from those exposed to UV-B+ Si-. Moreover, APX, H₂O₂, and MDA concentrations did not show any alterations for different UV-B and Si levels (Table 5). Hideg et al. (2013) and Kataria et al. (2014) concluded that UV-B promoted a greater activity of SOD and

CAT enzymes, a common mechanism to cope with UV-B in several plants. The higher concentration of H₂O₂ observed in the leaves of plants subjected to UV-B- Si+ indicate the role of this element as a defense-stimulating agent. Sewelam et al. (2014) highlighted that H₂O₂ is an important signaling molecule in plants, mediating several physiological and biochemical processes in plant cells.

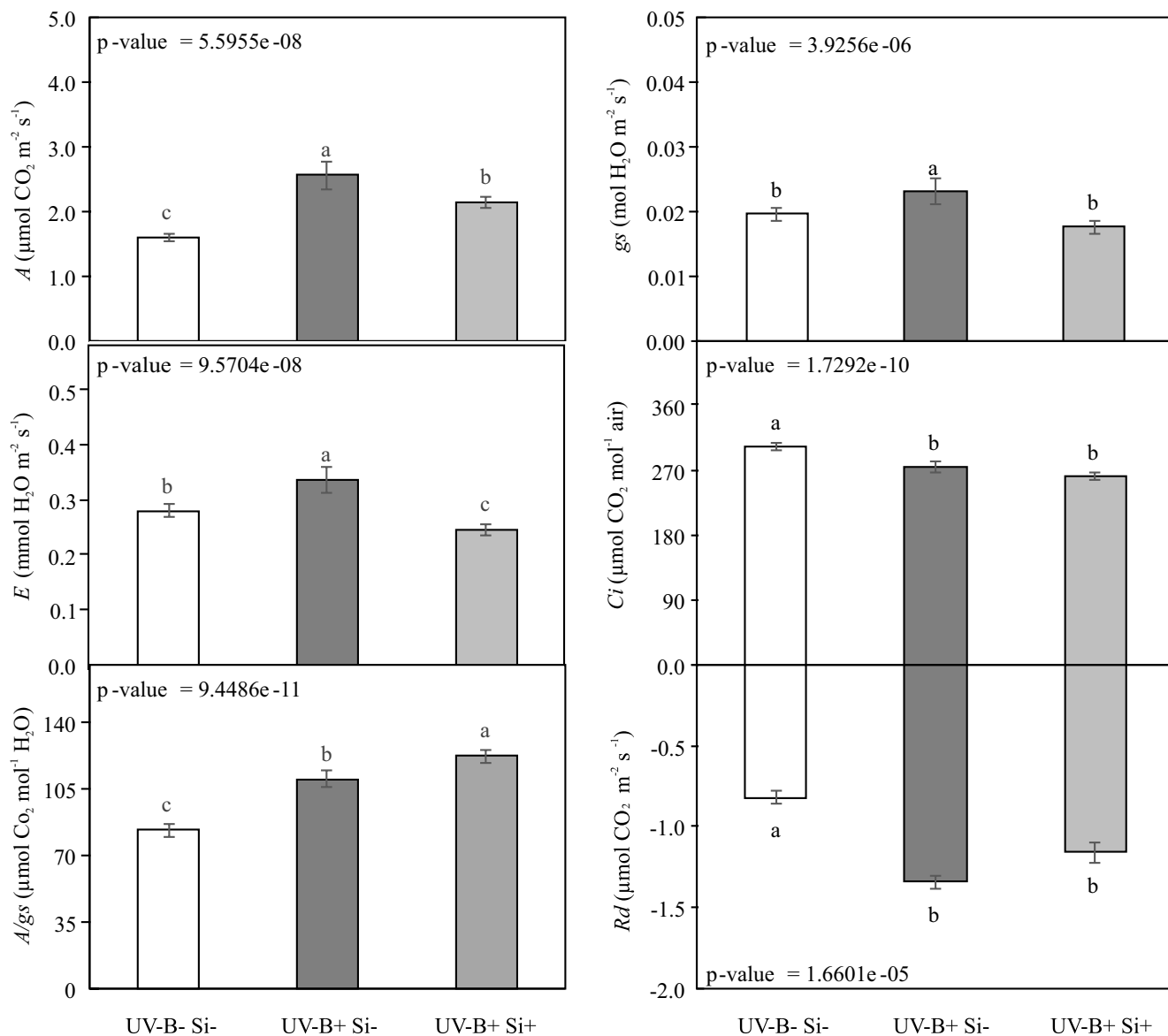


Figure 3. Effects of ultraviolet-B (UV-B) radiation and silicon on gas-exchange variables of plants of the Catongo cacao (*Theobroma cacao*) genotype, showing: A, net CO₂ assimilation rate (*A*); B, stomatal conductance (*g_s*); C, transpiration (*E*); D, CO₂ concentration in intercellular air spaces (*C_i*); E, water-use efficiency (*A/g_s*); and F, dark mitochondrial respiration rate (*R_d*). Equal letters do not differ by Tukey's test, at 5% probability. Bars represent the standard error of the mean (n = 5). UV-B-, 0.0 kJ m⁻² per day; UV-B+, 3.0 kJ m⁻² per day; Si-, 0.0 mmol L⁻¹; and Si+, 2.0 mmol L⁻¹.

Table 4. Effects of ultraviolet-B (UV-B) radiation and silicon on carbon-rich compounds (sucrose, total sugar, reducing sugars, lignin, and mucilage) in leaves of plants of the Catongo cacao (*Theobroma cacao*) genotype⁽¹⁾.

Variable	UV-B- Si-	UV-B+ Si-	UV-B+ Si+	p-value
Sucrose (mg g ⁻¹ DM)	3.79	4.59	5.09	0.27387
Total sugar (mg g ⁻¹ DM)	21.81 b	56.90 a	68.77 a	0.00034217
Reducing sugars (mg g ⁻¹ DM)	18.02 b	52.30 a	63.68 a	0.00027456
Lignin (mg g ⁻¹ DM)	42.81 b	45.75 a	46.56 a	0.00082561
Mucilage (%)	11.13 b	10.46 b	12.13 a	0.0010637

⁽¹⁾Means (n = 5) followed by equal letters do not differ by Tukey's test, at 5% probability. UV-B-, 0.0 kJ m⁻² per day; UV-B+, 3.0 kJ m⁻² per day; Si-, 0.0 mmol L⁻¹; Si+, 2.0 mmol L⁻¹; and DM, dry matter.

Table 5. Effects of ultraviolet-B (UV-B) radiation and silicon on antioxidant activity of the superoxide dismutase (SOD), catalase (CAT), and ascorbate peroxidase (APX) enzymes, as well as hydrogen peroxide (H₂O₂) and malondialdehyde (MDA) contents, in leaves of plants of the Catongo cacao (*Theobroma cacao*) genotype.

Variable	UV-B- Si-	UV-B+ Si-	UV-B+ Si+	p-value
SOD (SOD unit per g of DM)	23.73b	29.46ab	29.79a	0.030673
CAT (μmol H ₂ O ₂ per min per g of DM)	11.63b	16.62ab	18.46a	0.024049
APX (μmol ascorbate per min per g of DM)	0.0817	0.0979	0.0927	0.59992
H ₂ O ₂ (μmol H ₂ O ₂ per g of DM)	59.906	78.644	64.656	0.076612
MDA (nmol MDA per g of DM)	300.97	287.57	321.35	0.74278

⁽¹⁾Means (n = 5) followed by equal letters do not differ by Tukey's test, at 5% probability. UV-B-, 0.0 kJ m⁻² per day; UV-B+, 3.0 kJ m⁻² per day; Si-, 0.0 mmol L⁻¹; Si+, 2.0 mmol L⁻¹; and DM, dry matter.

Conclusion

In cacao (*Theobroma cacao*) plants, silicon application mitigates the damaging effects of UV-B, decreases the production of UVB-absorbing compounds, and reduces carbon consumption through cellular respiration, promoting energy saving.

References

- AEBI, H. Catalase *in vitro*. **Methods in Enzymology**, v.105, p.121-126, 1984. DOI: [https://doi.org/10.1016/S0076-6879\(84\)05016-3](https://doi.org/10.1016/S0076-6879(84)05016-3).
- ALEXIEVA, V.; SERGIEV, I.; MAPELLI, S.; KARANOV, E. The effect of drought and ultraviolet radiation on growth and stress markers in pea and wheat. **Plant, Cell & Environment**, v.24, p.1337-1344, 2001. DOI: <https://doi.org/10.1046/j.1365-3040.2001.00778.x>.
- ASADA, K. The water-water cycle in chloroplasts: scavenging of active oxygens and dissipation of excess photons. **Annual Review of Plant Physiology and Plant Molecular Biology**, v.50, p.601-639, 1999. DOI: <https://doi.org/10.1146/annurev.arplant.50.1.601>.
- BEGGS, C.J.; WELLMANN, E. Photocontrol of flavonoid biosynthesis. In: KENDRICK, R.E.; KRONENBERG, G.H.M. (Ed.). **Photomorphogenesis in plants**. Dordrecht: Springer, 1994. p.733-751. DOI: https://doi.org/10.1007/978-94-011-1884-2_26.
- BISWAS, D.K.; JANSEN, M.A.K. Natural variation in UV-B protection amongst *Arabidopsis thaliana* accessions. **Emirates Journal of Food and Agriculture**, v.24, p.621-631, 2012. DOI: <https://doi.org/10.9755/ejfa.v24i6.14681>.
- BONINO, R. **Joia rara da Bahia: conheça o cacao Catongo, preciosa variedade de amêndoa albina que promete valorizar a produção de chocolate fino brasileiro**. **Menu**, v.175, p.36-39, 2013.
- BUEGE, J.A.; AUST, S.D. Microsomal lipid peroxidation. **Methods in Enzymology**, v.52, p.302-310, 1978. DOI: [https://doi.org/10.1016/s0076-6879\(78\)52032-6](https://doi.org/10.1016/s0076-6879(78)52032-6).
- CUZZUOL, G.R.F.; GAMA, V.N.; ZANETTI, L.V.; WERNER, E.T.; PEZZOPANE, J.E.M. UV-B effects on growth, photosynthesis, total antioxidant potential and cell wall components of shade-tolerant and sun-tolerant ecotypes of *Paubrasilia echinata*. **Flora**, v.271, art.151679, 2020. DOI: <https://doi.org/10.1016/j.flora.2020.151679>.
- DAMATTA, F.M.; LOOS, R.A.; SILVA, E.A.; LOUREIRO, M.E. Limitations to photosynthesis in *Coffea canephora* as a result of nitrogen and water availability. **Journal of Plant Physiology**, v.159, p.975-981, 2002. DOI: <https://doi.org/10.1078/0176-1617-00807>.
- DU, Z.; BRAMLAGE, W.J. Modified thiobarbituric acid assay for measuring lipid oxidation in sugar-rich plant tissue extracts. **Journal of Agricultural and Food Chemistry**, v.40, p.1566-1570, 1992. DOI: <https://doi.org/10.1021/jf00021a018>.
- DUBOIS, M.; GILLES, K.A.; HAMILTON, J.K.; REBERS, P.A.; SMITH, F. Colorimetric method for determination of sugars and related substances. **Analytical Chemistry**, v.28, p.350-356, 1956. DOI: <https://doi.org/10.1021/ac60111a017>.
- GHANEM, M.E.; HAN, R.-M.; CLASSEN, B.; QUETIN-LECLERQ, J.; MAHY, G.; RUAN, C.-J.; QIN, P.; PÉREZ-ALFOCEA, F.; LUTTS, S. Mucilage and polysaccharides in the halophyte plant species *Kosteletzkya virginica*: localization and composition in relation to salt stress. **Journal of Plant**

- Physiology**, v.167, p.382-392, 2010. DOI: <https://doi.org/10.1016/j.jplph.2009.10.012>.
- EPSTEIN, E.; BLOOM, A.J. **Nutrição mineral de plantas: princípios e perspectivas**. 2.ed. Londrina: Planta, 2006. 403p.
- FENG, J.; SHI, Q.; WANG, X.; WEI, M.; YANG, F.; XU, H. Silicon supplementation ameliorated the inhibition of photosynthesis and nitrate metabolism by cadmium (Cd) toxicity in *Cucumis sativus* L. **Scientia Horticulturae**, v.123, p.521-530, 2010. DOI: <https://doi.org/10.1016/j.scienta.2009.10.013>.
- FORSTER, P.M.; THOMPSON, D.W.J.; BALDWIN, M.P.; CHIPPERFIELD, M.P.; DAMERIS, M.; HAIGH, J.D.; KAROLY, D.J.; KUSHNER, P.J.; RANDEL, W.J.; ROSENLOF, K.H.; SEIDEL, D.J.; SOLOMON, S. Stratospheric changes and climate. In: SCIENTIFIC Assessment of Ozone Depletion: 2010. Geneva: World Meteorological Organization, 2011. (Global Ozone Research and Monitoring Project-Report n° 52).
- GIANNOPOLITIS, C.N.; RIES, S.K. Superoxide dismutases. II. Purification and quantitative relationship with water-soluble protein in seedlings. **Plant Physiology**, v.59, p.315-318, 1977. DOI: <https://doi.org/10.1104/pp.59.2.315>.
- HIDEG, É.; JANSEN, M.A.K.; STRID, A. UV-B exposure, ROS, and stress: inseparable companions or loosely linked associates? **Trends in Plant Science**, v.18, p.107-115, 2013. DOI: <https://doi.org/10.1016/j.tplants.2012.09.003>.
- HOAGLAND, D.R.; ARNON, D.I. **The water-culture method for growing plants without soil**. Berkley: California Agricultural Experiment Station, 1950. (Circular-347).
- HOFMANN, R.W.; CAMPBELL, B.D. Leaf-level responses to ultraviolet-B radiation in *Trifolium repens* populations under defoliation pressure. **Environmental and Experimental Botany**, v.78, p.64-69, 2012. DOI: <https://doi.org/10.1016/j.envexpbot.2011.12.019>.
- JOHANSEN, D.A. **Plant microtechnique**. New York: McGraw-Hill, 1940. 530p.
- KAKANI, V.G.; REDDY, K.R.; ZHAO, D.; MOHAMMED, A.R. Effects of ultraviolet-B radiation on cotton (*Gossypium hirsutum* L.) morphology and anatomy. **Annals of Botany**, v.91, p.817-826, 2003a. DOI: <https://doi.org/10.1093/aob/mcg086>.
- KAKANI, V.G.; REDDY, K.R.; ZHAO, D.; SAILAJA, K. Field crop responses to ultraviolet-B radiation: a review. **Agricultural and Forest Meteorology**, v.120, p.191-218, 2003b. DOI: <https://doi.org/10.1016/j.agrformet.2003.08.015>.
- KANG, J.; ZHAO, W.; ZHU, X. Silicon improves photosynthesis and strengthens enzyme activities in the C3 succulent xerophyte *Zygophyllum xanthoxylum* under drought stress. **Journal of Plant Physiology**, v.199, p.76-86, 2016. DOI: <https://doi.org/10.1016/j.jplph.2016.05.009>.
- KATARIA, S.; GURUPRASAD, K.N. Exclusion of solar UV components improves growth and performance of *Amaranthus tricolor* varieties. **Scientia Horticulturae**, v.174, p.36-45, 2014. DOI: <https://doi.org/10.1016/j.scienta.2014.05.003>.
- KATARIA, S.; JAJOO, A.; GURUPRASAD, K.N. Impact of increasing ultraviolet-B (UV-B) radiation on photosynthetic processes. **Journal of Photochemistry and Photobiology B: Biology**, v.137, p.55-66, 2014. DOI: <https://doi.org/10.1016/j.jphotobiol.2014.02.004>.
- KORNDÖRFER, G.H.; PEREIRA, H.S.; NOLLA, A. **Análise de silício: solo, planta e fertilizante**. Uberlândia: GPSi-ICIAG-UFU, 2004. 34p. (Boletim técnico, 2).
- LAMBERS, H.; POORTER, H. Inherent variation in growth rate between higher plants: a search for physiological causes and ecological consequences. **Advances in Ecological Research**, v.23, p.87-261, 1992. DOI: [https://doi.org/10.1016/S0065-2504\(08\)60148-8](https://doi.org/10.1016/S0065-2504(08)60148-8).
- LENNON, A.M.; LEWIS, V.R.; FARRELL, A.D.; UMAHARAN, P. Photochemical responses to light in sun and shade leaves of *Theobroma cacao* L. (West African Amelonado). **Scientia Horticulturae**, v.276, art.109747, 2021. DOI: <https://doi.org/10.1016/j.scienta.2020.109747>.
- LICHTENTHALER, H.K.; BUSCHMANN, C. Chlorophylls and carotenoids: measurement and characterization by UV-VIS spectroscopy. **Current Protocols in Food Analytical Chemistry**, v.1, F4-3.1-F4.3.8, 2001. DOI: <https://doi.org/10.1002/0471142913.faf0403s01>.
- LIMA, A.L.S.; DAMATTA, F.M.; PINHEIRO, H.A.; TOTOLA, M.R.; LOUREIRO, M.E. Photochemical responses and oxidative stress in two clones of *Coffea canephora* under water deficit conditions. **Environmental and Experimental Botany**, v.47, p.239-247, 2002. DOI: [https://doi.org/10.1016/S0098-8472\(01\)00130-7](https://doi.org/10.1016/S0098-8472(01)00130-7).
- LOBO, F. de A.; BARROS, M.P. de; DALMAGRO, H.J.; DALMOLIN, Â.C.; PEREIRA, W.E.; SOUZA, Ê.C. de; VOURLITIS, G.L.; RODRÍGUEZ ORTÍZ, C.E. Fitting net photosynthetic light-response curves with Microsoft Excel – a critical look at the models. **Photosynthetica**, v.51, p.445-456, 2013. DOI: <https://doi.org/10.1007/s11099-013-0045-y>.
- LOGAN, B.A.; ADAMS III, W.W.; DEMMIG-ADAMS, B. Avoiding common pitfalls of chlorophyll fluorescence analysis under field conditions. **Functional Plant Biology**, v.34, p.853-859, 2007. DOI: <https://doi.org/10.1071/FP07113>.
- MARTINEZ, C.A.; LOUREIRO, M.E.; OLIVA, M.A.; MAESTRI, M. Differential responses of superoxide dismutase in freezing resistant *Solanum curtilobum* and freezing sensitive *Solanum tuberosum* subjected to oxidative and water stress. **Plant Science**, v.160, p.505-515, 2001. DOI: [https://doi.org/10.1016/s0168-9452\(00\)00418-0](https://doi.org/10.1016/s0168-9452(00)00418-0).
- MARTÍNEZ-LÜSCHER, J.; MORALES, F.; DELROT, S.; SÁNCHEZ-DÍAZ, M.; GOMÈS, E.; AGUIRREOLEA, J.; PASCUAL, I. Characterization of the adaptive response of grapevine (cv. Tempranillo) to UV-B radiation under water deficit conditions. **Plant Science**, v.232, p.13-22, 2015. DOI: <https://doi.org/10.1016/j.plantsci.2014.12.013>.
- MENGARDA, L.H.G.; MILANEZ, C.R.D.; SILVA, D.M.; AGUILAR, M.A.G.; CUZZUOL, G.R.F. Morphological and physiological adjustments of Brazilwood (*Caesalpinia echinata* Lam.) to direct solar radiation. **Brazilian Journal of Plant Physiology**, v.24, p.161-172, 2012. DOI: <https://doi.org/10.1590/S1677-04202012000300003>.
- MESSINGER, D.J.; MCLEOD, A.R.; FRY, S.C. The role of ultraviolet radiation, photosensitizers, reactive oxygen species and ester groups in mechanisms of methane formation from pectin. **Plant, Cell & Environment**, v.32, p.1-9, 2009. DOI: <https://doi.org/10.1111/j.1365-3040.2008.01892.x>.

- MING, D.F.; PEI, Z.F.; NAEEM, M.S.; GONG, H.J.; ZHOU, W.J. Silicon alleviates PEG-induced water-deficit stress in upland rice seedlings by enhancing osmotic adjustment. **Journal of Agronomy and Crop Science**, v.198, p.14-26, 2012. DOI: <https://doi.org/10.1111/j.1439-037X.2011.00486.x>.
- NAKANO, Y.; ASADA, K. Hydrogen peroxide is scavenged by ascorbate-specific peroxidase in spinach chloroplasts. **Plant and Cell Physiology**, v.22, p.867-880, 1981. DOI: <https://doi.org/10.1093/oxfordjournals.pcp.a076232>.
- NAKAYAMA, L.H.I.; SOARES, M.K.M.; APPEZZATO-DA-GLÓRIA, B. Contribuição ao estudo anatômico da folha e do caule do cacauero (*Theobroma cacao* L.). **Scientia Agricola**, v.53, p.73-73, 1996. DOI: <https://doi.org/10.1590/S0103-90161996000100010>.
- PARK, Y.K.; IKEGAKI, M.; ABREU, J.A. da S.; ALCICI, N.M.F. Estudo da preparação dos extratos de própolis e suas aplicações. **Food Science and Technology**, v.18, p.313-318, 1998. DOI: <https://doi.org/10.1590/S0101-20611998000300011>.
- R CORE TEAM. **R: a language and environment for statistical computing**. Vienna: R Foundation for Statistical Computing, 2021. Available at: <https://www.R-project.org>. Accessed on: July 24 2023.
- RIVAI, R.R.; MIYAMOTO, T.; AWANO, T.; YOSHINAGA, A.; CHEN, S.; SUGIYAMA, J.; TOBIMATSU, Y.; UMEZAWA, T.; KOBAYASHI, M. Limiting silicon supply alters lignin content and structures of sorghum seedling cell walls. **Plant Science**, v.321, art.111325, 2022. DOI: <https://doi.org/10.1016/j.plantsci.2022.111325>.
- RUHLAND, C.T.; XIONG, F.S.; CLARK, W.D.; DAY, T.A. The influence of ultraviolet-B radiation on growth, hydroxycinnamic acids and flavonoids of *Deschampsia antarctica* during springtime ozone depletion in Antarctica. **Photochemistry and Photobiology**, v.81, p.1086-1093, 2005. DOI: <https://doi.org/10.1562/2004-09-18-RA-321>.
- RUUHOLA, T.; NYBAKKEN, L.; RANDRIAMANANA, T.; LAVOLA, A.; JULKUNEN-TIITTO, R. Effects of long-term UV-exposure and plant sex on the leaf phenoloxidase activities and phenolic concentrations of *Salix myrsinifolia* (Salisb.). **Plant Physiology and Biochemistry**, v.126, p.55-62, 2018. DOI: <https://doi.org/10.1016/j.plaphy.2018.02.025>.
- SANKARI, M.; HRIDYA, H.; SNEHA, P.; DOSS, C.G.P.; RAMAMOORTHY, S. Effect of UV radiation and its implications on carotenoid pathway in *Bixa orellana* L. **Journal of Photochemistry & Photobiology, B: Biology**, v.176, p.136-144, 2017. DOI: <https://doi.org/10.1016/j.jphotobiol.2017.10.002>.
- SANTOS, W.D. dos; FERRARESE, M.L.L.; NAKAMURA, C.V.; MOURÃO, K.S.M.; MANGOLIN, C.A.; FERRARESE-FILHO, O. Soybean (*Glycine max*) root lignification induced by ferulic acid. The possible mode of action. **Journal of Chemical Ecology**, v.34, p.1230-1241, 2008. DOI: <https://doi.org/10.1007/s10886-008-9522-3>.
- SCHÄDEL, C.; BLOCHL, A.; RICHTER, A.; HOCH, G. Quantification and monosaccharide composition of hemicelluloses from different plant functional types. **Plant Physiology and Biochemistry**, v.48, p.1-8, 2010. DOI: <https://doi.org/10.1016/j.plaphy.2009.09.008>.
- SEWELAM, N.; JASPERT, N.; VAN DER KELEN, K.; TOGNETTI, V.B.; SCHMITZ, J.; FRERIGMANN, H.; STAHL, E.; ZEIER, J.; VAN BREUSEGEM, F.; MAURINO, V.G. Spatial H₂O₂ signaling specificity: H₂O₂ from chloroplasts and peroxisomes modulates the plant transcriptome differentially. **Molecular Plant**, v.7, p.1191-1210, 2014. DOI: <https://doi.org/10.1093/mp/ssu070>.
- SINGLETON, V.L.; ROSSI, J.A. Colorimetry of total phenolics with phosphomolybdic- phosphotungstic acid reagents. **American Journal of Enology and Viticulture**, v.16, p.144-158, 1965. DOI: <https://doi.org/10.5344/ajev.1965.16.3.144>.
- SCHNEIDER, C.A.; RASBAND, W.S.; ELICEIRI, K.W. NIH Image to ImageJ: 25 years of image analysis. **Nature Methods**, v.9, p.671-675, 2012. DOI: <https://doi.org/10.1038/nmeth.2089>.
- VERDAGUER, D.; LLORENS, L.; BERNAL, M.; BADOSA, J. Photomorphogenic effects of UVB and UVA radiation on leaves of six Mediterranean sclerophyllous woody species subjected to two different watering regimes at the seedling stage. **Environmental and Experimental Botany**, v.79, p.66-75, 2012. DOI: <https://doi.org/10.1016/j.envexpbot.2012.01.008>.
- WONG, T.M.; SULLIVAN, J.H.; EISENSTEIN, E. Acclimation and compensating metabolite responses to UV-B radiation in natural and transgenic *Populus* spp. defective in lignin biosynthesis. **Metabolites**, v.12, art.767, 2022. DOI: <https://doi.org/10.3390/metabo12080767>.
- YAGHUBI, K.; GHADERI, N.; VAFAEE, Y.; JAVADI, T. Potassium silicate alleviates deleterious effects of salinity on two strawberry cultivars grown under soilless pot culture. **Scientia Horticulturae**, v.213, p.87-95, 2016. DOI: <https://doi.org/10.1016/j.scienta.2016.10.012>.
- YAO, X.; CHU, J.; CAI, K.; LIU, L.; SHI, J.; GENG, W. Silicon improves the tolerance of wheat seedlings to ultraviolet-B stress. **Biological Trace Element Research**, v.143, p.507-517, 2011. DOI: <https://doi.org/10.1007/s12011-010-8859-y>.
- YAO, X.; LIU, Q. Changes in morphological, photosynthetic and physiological responses of Mono Maple seedlings to enhanced UV-B and to nitrogen addition. **Plant Growth Regulation**, v.50, p.165-177, 2006. DOI: <https://doi.org/10.1007/s10725-006-9116-4>.
- ZANETTI, L.V.; MILANEZ, C.R.D.; GAMA, V.N.; AGUILAR, M.A.G.; SOUZA, C.A.S.; CAMPOSTRINI, E.; FERRAZ, T.M.; FIGUEIREDO, F.A.M.M. de A. Leaf application of silicon in young cacao plants subjected to water deficit. **Pesquisa Agropecuária Brasileira**, v.51, p.215-223, 2016. DOI: <https://doi.org/10.1590/S0100-204X2016000300003>.
- ZHU, Y.-X.; XU, X.-B.; HU, Y.-H.; HAN, W.-H.; YIN, J.-L.; LI, H.-L.; GONG, H.-J. Silicon improves salt tolerance by increasing root water uptake in *Cucumis sativus* L. **Plant Cell Reports**, v.34, p.1629-1646, 2015. DOI: <https://doi.org/10.1007/s00299-015-1814-9>.